

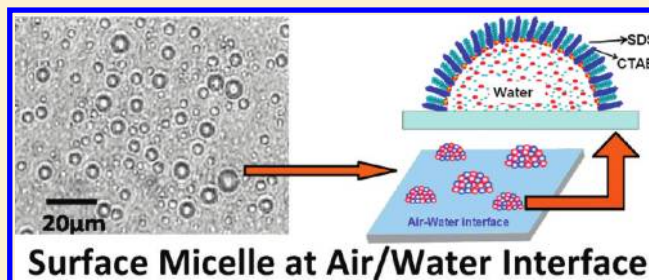
# Aggregation Behavior of SDS/CTAB Catanionic Surfactant Mixture in Aqueous Solution and at the Air/Water Interface

Bidisha Tah, Prabir Pal, Mrityunjoy Mahato, and G. B. Talapatra\*

Department of Spectroscopy, Indian Association for the Cultivation of Science, Jadavpur, Kolkata-700 032, India

**S** Supporting Information

**ABSTRACT:** Herein, we report the aggregation behavior of catanionic mixtures of the anionic surfactant sodium dodecyl sulfate (SDS) and the cationic surfactant cetyltrimethylammonium bromide (CTAB) in solution and at the air/water interface obtained by the Langmuir–Blodgett (LB) technique. We employed Fourier transform infrared spectroscopy, in situ phase-contrast inverted microscopy, scanning electron microscopy, and atomic force microscopy to characterize the systems in solution, at the air/water interface, and in LB films. We found spherical vesicles at the SDS/CTAB ratio of 35/65 in aqueous solution and an ordered aggregated morphology called surface micelles at SDS/CTAB ratios of 35/65 to 65/35 at the air/water interface. Other mixtures (SDS/CTAB = 90/10, 10/90) were found to contain mostly disordered aggregated microstructures. An in situ time-dependent study of surface micelle formation at the air/water interface showed micelle ripening through the fusion of smaller micelles. These micelles were successfully immobilized on a glass substrate by the LB technique. Overall, the study might find application in the fundamental science of the physical chemistry of surfactant systems, as well as in the preparation of drug delivery system.



## 1. INTRODUCTION

Recently, surfactants have been of tremendous scientific importance because of their many promising applications in detergents, cosmetics, material fabrication, and drug delivery, among other areas.<sup>1–4</sup> In addition, several fundamental scientific interests lie behind surfactant systems in the fields of physical chemistry and biology.<sup>5,6</sup> The main property of surfactant systems is that their aggregation phenomena arise from various noncovalent interactions (such as  $\pi$ – $\pi$  stacking, H-bonding, van der Waals interactions) operating at the molecular level.<sup>1,7</sup>

In this respect, a fascinating catanionic binary surfactant system has been drawing much attention because of the tunability of its oppositely charged head groups.<sup>8,9</sup> Mixtures of cationic and anionic surfactants can form several types of aggregated microstructures such as vesicles, lamellar phases, precipitates, spheres, and rodlike structures.<sup>10,11</sup> According to Sohrabi et al.,<sup>12</sup> the phase behavior of cationic/anionic surfactant mixtures depends on the actual concentrations of the surfactants, the lengths of their alkyl chains, the temperature, and the molar ratio. In a pure surfactant, the repulsive electrostatic interaction between two similarly charged head groups increases the free energy to form micelles.<sup>13</sup> On the other hand, in catanionic mixtures, the electrostatic interaction between two oppositely charged head groups decreases the free energy to form stable catanionic vesicles, without any high-energy methods such as sonication and extrusion.<sup>14–16</sup>

Mixtures of the anionic surfactant sodium dodecyl sulfate (SDS) and the cationic surfactant cetyltrimethylammonium bromide (CTAB) are important to study at the air/water interface

because of their relevance in diverse areas of fundamental chemistry.<sup>17</sup> Studies on pure surfactants as well as surfactant mixtures are also important regarding their reactive and thermodynamic processes leading to various kinds of self-assembled structures/products.<sup>18,19</sup> The Langmuir–Blodgett (LB) technique can facilitate the study of the surface morphologies of different types of aggregated structures.<sup>20–22</sup> The vesiculation, cracking, buckling, folding, and collapse of surfactant monolayers have been well studied by this technique.<sup>23</sup> Our laboratory has also performed many of such studies.<sup>20,24–28</sup> Despite the many studies on surfactant mixtures<sup>10,29,30</sup> regarding their surface behavior and assembly, the exact natures of the molecular interactions and the aggregation behavior are still not fully understood.

Considering the enormous industrial and biological importance of surfactants, the present work was undertaken with the primary aim of studying the aggregation behavior of the catanionic system SDS/CTAB with varying compositions in aqueous solution as well as in LB films. To confirm the self-assembled structures formed by interactions between the cationic and anionic surfactants, Fourier transform infrared (FTIR) spectroscopy was used. Phase-contrast inverted microscopy (PCIM) was also employed for in situ imaging in aqueous solution and at the air/water interface. Here, the LB technique allows for the study of both the aggregation behavior and the surface properties of the

**Received:** March 18, 2011

**Revised:** April 28, 2011

**Published:** June 15, 2011

formed aggregates at the air/water interface and in LB films. In addition, high-resolution field-emission scanning electron microscopy (FE-SEM) and atomic force microscopy (AFM) were used to study the systems in LB films.

## 2. EXPERIMENTAL SECTION

**2.1. Materials.** The anionic surfactant sodium dodecyl sulfate and the cationic surfactant cetyltrimethylammonium bromide were purchased from Sigma Chemical Co. (St. Louis, MO; purity 99%) and Himedia Laboratories Pvt. Ltd. (Mumbai, India; purity >98%), respectively. Chloroform (UV grade) and methanol were purchased from Spectrochem (Mumbai, India) and Merck (Darmstadt, Germany), respectively.

**2.2. Sample Preparation.** *2.2.1. Preparation of Stock Solutions.* A stock solution of SDS with a concentration of 0.26 mg/mL was prepared in 1:1 chloroform/methanol solvent, and a solution of CTAB with a concentration of 0.26 mg/mL was prepared in chloroform solvent. For catanionic surfactants, the solutions of SDS and CTAB were mixed in specific volume ratios. The concentrations of the solutions of pure SDS and CTAB were 0.913 and 0.714 mM, respectively, which were far below than their critical micelle concentrations (CMCs).<sup>31,32</sup>

*2.2.2. Preparation of Vesicles.* The prepared catanionic solution in organic solvent was heated in a water bath at 70 °C to evaporate the solvent. Then, Millipore water was added to allow the formation of vesicles.<sup>33</sup>

*2.2.3. Preparation of Thin Layers of Vesicular Aqueous Solutions.* One or two drops of the catanionic vesicular aqueous solution prepared as described in the preceding section were dropped onto a hydrophilic glass substrate and covered with a fine glass coverslip. A water film, that is, a layer of catanionic vesicular solution in aqueous medium, was thus prepared between glass coverslips.

**2.3. Methods.** *2.3.1. Surface Pressure–Area ( $\pi$ –A) Isotherm Measurements.* For surface pressure–area ( $\pi$ –A) isotherm measurements of pure anionic systems, pure cationic systems, and different ratios of catanionic mixtures on a water subphase, stock solutions were prepared. Different solutions of surfactants were spread on the water subphase at a particular temperature (28 °C) that was above than the Kraft temperatures of both surfactants.<sup>34</sup> The spreading was done using a microsyringe (Hamilton Bonaduz AG, Bonaduz, Switzerland) in such a manner that the surface pressure did not rise above 0.5 mN/m. The numbers of molecules thus spread for pure SDS and CTAB were calculated using their molecular weights as 288.38 and 364.46, respectively. On the other hand, for the mixed surfactants, the number of molecules was represented by the mean molecular weight ( $M$ ) as follows

$$M = \frac{M_1 c_1 v_1 + M_2 c_2 v_2}{c_1 v_1 + c_2 v_2} \quad (1)$$

where  $M_1$  and  $M_2$  are the molecular weights,  $c_1$  and  $c_2$  are the concentrations (in mM), and  $v_1$  and  $v_2$  are the volume percentages of first and second samples, respectively. In general, the monolayer was allowed to stabilize for 10–15 min and then slowly compressed with a compression speed of 1 Å<sup>2</sup>/(molecule min).

The computerized LB trough used was a Teflon-barrier type (model LB2007DC, Apex Instruments Co., Kolkata, India) enclosed in a plexiglass box to reduce film contamination. It was equipped with a Wilhelmy-type balance with an accuracy of  $\pm 0.01$  mN/m. The trough width and length were 200 and 600 mm, respectively. The subphase water with a pH of 5.5

and a resistivity of 18.2 M $\Omega$  cm was prepared using a Milli-Q apparatus through an ELIX system from Millipore (Billerica, MA). All experiments were performed at a temperature of 28  $\pm$  1 °C unless otherwise mentioned. At least three independent runs were performed to check the reproducibility.

*2.3.2. Surface Pressure–Time ( $\pi$ – $t$ ) Kinetics at the Air/Water Interface.* Solutions of different compositions of catanionic mixtures (SDS/CTAB = 90/10, 65/35, 50/50, 35/65, and 10/90) in organic solvent were used to study the adsorption growth kinetics. A fixed number of molecules was spread on a water subphase with an area of 400 cm<sup>2</sup> (20 cm  $\times$  20 cm) to observe the change in  $\pi$ – $t$  kinetics.

*2.3.3. Process of Substrate Cleaning.* All substrates (glass and silicon wafer) were cleaned in a liquid-soap ultrasonic bath and then repeatedly rinsed with Millipore water. They were then immersed in acetone in an ultrasonic bath. Finally, they were cleaned using Millipore water in the ultrasonic bath. A uniform layer of water on the slide confirmed the hydrophilicity of the slide.<sup>14</sup>

*2.3.4. Preparations of LB and Cast Films.* Monolayers prepared at the air/water interface were transferred very carefully through an upstroke with a speed of 5 mm/min at constant surface pressure (20 mN/m) onto hydrophilic glass coverslips that had previously been immersed in the subphase. Cast films were prepared by drop casting the vesicular aqueous solution onto a hydrophilic substrate.<sup>25</sup>

*2.3.5. FE-SEM and AFM Characterizations.* A high-resolution field-emission scanning electron microscope (model JEOL JSM-6700 F, Tokyo, Japan) with a range of 0.5–30 kV and a lateral resolution of 1.2–2.2 nm was employed to extract the surface morphology of all transferred LB films and those on the fine hydrophilic glass substrate.

For study the surface morphology of the LB films, AFM (Veeco diCP-II model AP-0100, England) imaging was used. The tapping mode was used in air to minimize any kind of force exerted on the samples from the scanning tip. A thin phosphorus-doped silicon cantilever (with no coating on the front side and a 50  $\pm$  10 nm aluminum coating on the backside) with a resistivity of 1–10  $\Omega$  cm was used for scanning. The thickness of the cantilever ranged from 3.5 to 4.5  $\mu$ m, the length was 115–135  $\mu$ m, and the width was 30–40  $\mu$ m. The processed images were subsequently analyzed for diameter, height, and surface roughness by ProScan 1.8 and Image Analysis 2.1 software. Line profiles were used to calculate the surface roughness. The height profile showed the variation between the highest peak and lowest valley along the line.

*2.3.6. FTIR Spectroscopy.* FTIR spectra of cast films of pure and mixed surfactants on silicon wafers were recorded at room temperature by with a Series II Magna-IR model 750 spectrometer from Nicolet Instrument Corporation (Madison, WI). In all cases, the data were averaged over 100 scans. The resolution of the instrument was 4 cm<sup>–1</sup>.

*2.3.7. Imaging on a Phase-Contrast Inverted Microscope.* Self-assembly of catanionic surfactants in aqueous solution and at the air/water interface were studied with a phase-contrast inverted microscope (Motic model AE31 fitted with a MINI-LB2006C LB film deposition system; Apex Instruments Co., Kolkata, India). Thin layers of uniform thickness of the aqueous solutions of catanionic surfactants between two coverslips were placed in the field of the microscope for observation of the features of different catanionic compositions. Moreover, we tried to use PCIM to observe the different assemblies with different composition ratios at the air/water interface after the

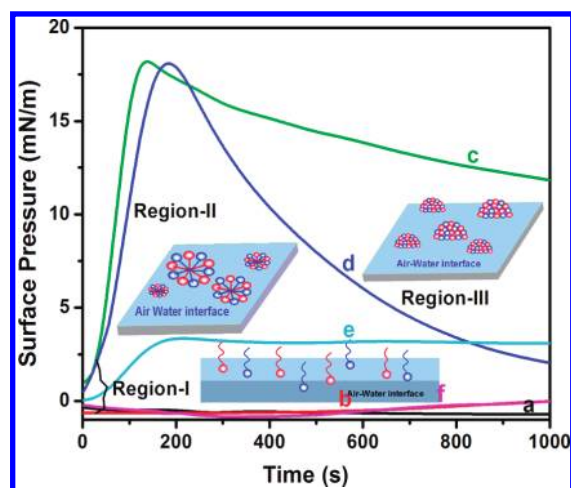


**Figure 1.** Surface pressure–time ( $\pi$ – $t$ ) kinetics data of SDS/CTAB spread at various compositions at the air/water interface. Curves a–f represent SDS/CTAB compositions of 0/100, 10/90, 35/65, 50/50, 65/35, and 90/10, respectively. Cartoon pictures show the probable self-assembly behaviors in regions I, II, and III.

premixed catanionic solutions in organic solvent had been spread on the trough.

### 3. RESULTS AND DISCUSSION

**3.1. Characteristics of Langmuir Monolayer of Pure Surfactants and Their Mixtures.** Stock solutions of pure SDS and CTAB having the same concentration (0.26 mg/mL) were prepared in volatile organic solvents and mixed in different volume ratios (SDS/CTAB = 90/10, 75/25, 65/35, 50/50, 35/65, 25/75, 10/90) to form catanionic solutions. These mixtures were spread on the water subphase. Figure 1 displays the surface activities, that is, the variations of surface pressure ( $\pi$ ) with time ( $t$ ), of different catanionic mixtures of SDS/CTAB.

This figure shows some interesting results about various anionic/cationic mixtures. For the cases of pure surfactants and for the extremely cationic-rich (SDS/CTAB = 10/90, curve b) and anionic-rich (SDS/CTAB = 90/10, curve f) compositions, the surface pressure remained almost zero. In these cases, the numbers of catanionic complexes were very low, and the rest of the molecules were free surfactants soluble in the subphase. Therefore, there was not much of growth in surface pressure. On the other hand, for the remaining compositions [namely, SDS/CTAB = 35/65 (curve c), 50/50 (curve d), and 65/35 (curve e)], the  $\pi$ – $t$  curves pass through a peak. Initially,  $\pi$  increases for a while before it decreases. The rates of increment and decrement of the surface pressure are different for the different compositions. From these observations, it can be concluded that, just after the spreading of the surfactant mixture, both surfactants have a tendency to sink into the subphase because of their solubility in water.<sup>23,35</sup> Over time, the electrostatic interaction between the two oppositely charged head groups plays a role in the formation of some catanionic complexes that are insoluble in water. These interaction processes are dynamic in nature.

The difference in the nature of  $\pi$ – $t$  curves for the two compositions SDS/CTAB = 35/65 (curve c) and 65/35 (curve e) arises because of the different numbers of cationic and anionic molecules having different degrees of solubility. According to Sohrabi et al, CTAB is more surface-active than SDS,<sup>12</sup> and

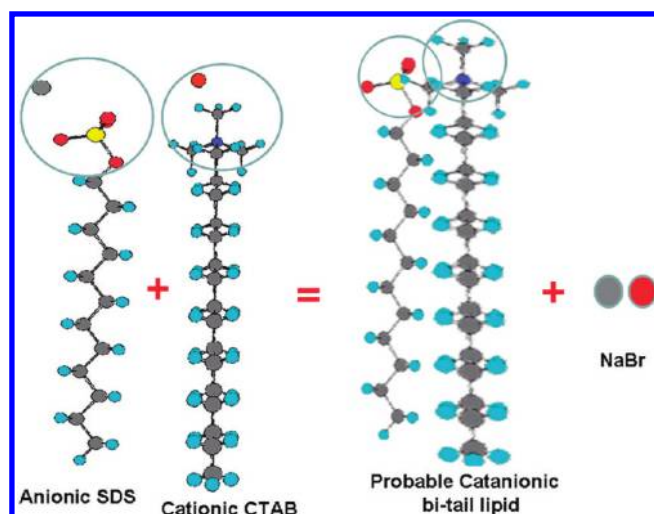


**Figure 2.** Illustration showing the conceptual equivalence between a mixture of cationic and anionic surfactants and bitail lipid molecules.

therefore, the CTAB molecules have a greater probability than the SDS molecules to reside at the surface. For the composition SDS/CTAB = 35/65, then, the number of CTAB molecules is higher, and these molecules mostly reside at or near the surface. These cationic CTAB molecules try to minimize their electrostatic repulsive force (i.e., free energy) and attract the anionic SDS molecules at the surface. Finally, they form some catanionic complex structures at the air/water interface and, in effect, increase the surface pressure. In contrast, for SDS/CTAB = 65/35, the concentration of CTAB molecules is less than that of SDS molecules, and the number of catanionic complexes at the air/water interface is lower. For this reason, the growth of surface pressure is less than for SDS/CTAB = 35/65. In the case of SDS/CTAB = 50/50, the number of catanionic complexes is less than for SDS/CTAB = 35/65 but higher than for SDS/CTAB = 65/35, and in effect, the graph for this composition lies between curves c and e. In CTAB, the headgroup is  $-\text{N}^+(\text{CH}_3)_3$  (trimethylammonium), whereas in SDS, the headgroup is  $\text{O}-\text{SO}_3^-$  (sulfate).<sup>12</sup> There is an electrostatic interaction between the positively and negatively charged head groups. Insolubility arises because of neutralization of the head-group charges and formation of a bitail structure. A probable scheme for the formation of the catanionic bitail structure is shown in Figure 2. Different composition ratios of anionic/cationic mixtures (SDS/CTAB) have different amounts of residual charges, which might be responsible for the different types of aggregates formed. The involvement of a repulsive steric hydration force cannot be ruled out for the stabilization of these structures.<sup>36</sup>

After the complexes have formed, they reach the surface and, over time, form definite two-dimensional assemblies at the air/water interface. Growth of the surface pressure indicates this phenomenon. The peak of the  $\pi$ – $t$  curve represents the maximum number of two-dimensional assemblies. As time passes, the two-dimensional structures start to convert into three-dimensional structures (hill-like) through reorganization, causing the decrement of the surface pressure. In contrast, in the case of SDS/CTAB = 65/35 (curve e), stable two-dimensional structures are formed, and the  $\pi$ – $t$  curve remains constant with time. In the case of three-dimensional alignment, the hydrophobic groups are exposed to the air, and the hydrophilic heads pull water



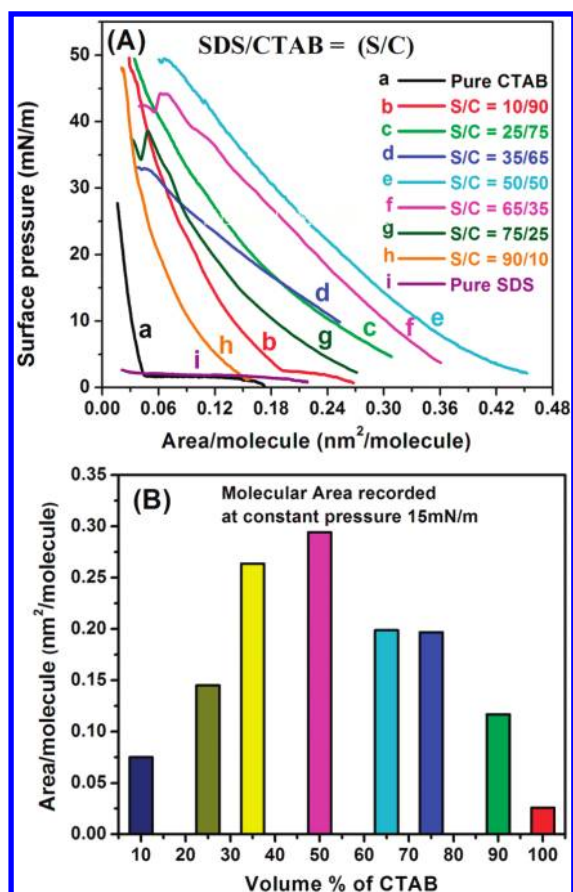


**Figure 3.** (A) Pressure–area ( $\pi$ – $A$ ) isotherms of the SDS/CTAB catanionic mixture surfactant with different compositions. (B) Plot of the change in molecular area with the volume fraction of one pure component (CTAB).

from the water subphase and form hill-like structures. Cartoons in Figure 1 depict the probable processes involved in different concentration ranges and in different time domains.

Figure 3A shows the pressure–area ( $\pi$ – $A$ ) isotherms of different compositions of catanionic surfactant at fixed temperature (28 °C). Here, the mean area per molecule represents the total area occupied divided by the total number of molecules.<sup>37,38</sup> We chose a premixing procedure to form a completely miscible component as mentioned in some literature reports.<sup>30,39</sup> The compression was done after allowing 10 min for the solvent to evaporate. It is clear from the Figure 3A that the two pure surfactants have distinct surface behaviors (curves a and i). The anionic SDS is reported to be soluble and could not form a stable Langmuir monolayer at the air/water interface, as evidenced by the absence of a buildup of surface pressure upon compression.<sup>23</sup> However, more interestingly, for CTAB, even though there is a buildup of surface pressure with compression, the onset area decreases with increasing waiting time, as shown in the Supporting Information (Figure 1). This behavior might arise because of the some extent of solubility of CTAB in water with time or self-organization due to the head-group interaction with the bulk water molecules.<sup>35</sup> The isotherms of binary systems indicate that they are more stable and surface-active than their pure counterparts. Interestingly, the natures of the isotherms vary with the composition of binary systems (i.e., the ratio of cationic and anionic surfactants). These changes might arise because of changes

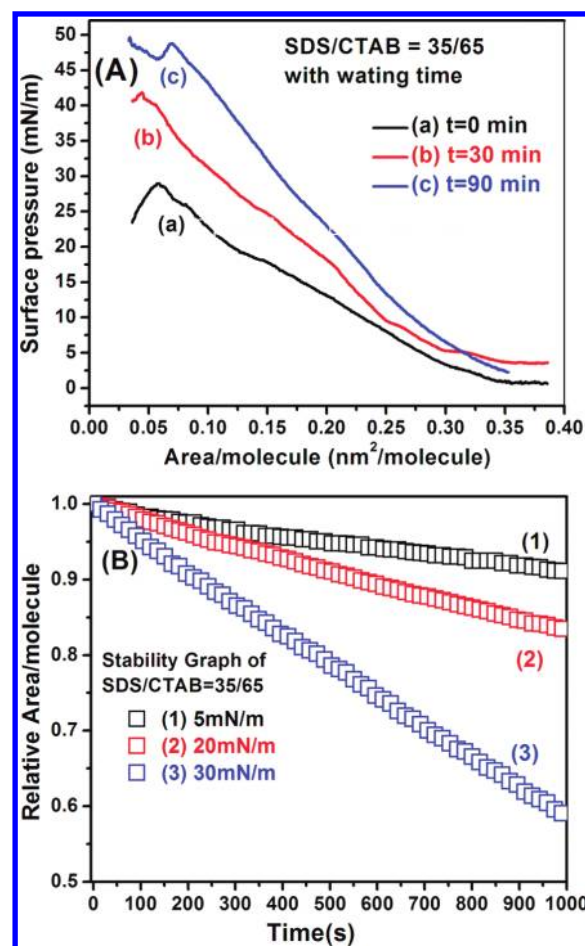


**Figure 4.** (A) Pressure–area ( $\pi$ – $A$ ) isotherm of the composition SDS/CTAB = 35/65 after different waiting times. (B) Stability curves of SDS/CTAB = 35/65 at different surface pressures.

in dissolution activity, surface activity, and so on. Moreover, the process of some self-assembly due to electrostatic interactions between cationic and anionic head groups might also be responsible for this behavior.<sup>37</sup>

Figure 3B explores the change in surface area with changing composition (increasing volume percentages of CTAB) at a surface pressure of 15 mN/m. The 1:1 composition of SDS/CTAB achieved the highest surface area/molecule (0.294 nm<sup>2</sup>/molecule), whereas the extremely cationic-rich (SDS/CTAB = 10/90) or anionic-rich (SDS/CTAB = 90/10) mixtures showed the lowest surface areas of 0.117 and 0.075 nm<sup>2</sup>/molecule, respectively. The surface area/molecule of the remaining compositions (SDS/CTAB = 65/35, 35/65, and 25/75) were found to lie in the neighboring region of the peak shown in the Figure 3B, namely, at 0.264, 0.199, and 0.197 nm<sup>2</sup>/molecule, respectively. This observation implies that, for these three mixtures, molecules are retained at the surface and might form some aggregates. Again, careful examination of Figure 3A shows that the nature of the  $\pi$ – $A$  isotherm for SDS/CTAB = 35/65 is slightly different from that for the other compositions. In this case, the collapse pressure is the lowest among the compositions. This might be related to its tendency to form three-dimensional structures upon compression.<sup>29</sup> Moreover, this shows the highest growth in surface pressure among the  $\pi$ – $t$  curves. These observations clearly indicate that this composition has a tendency to form

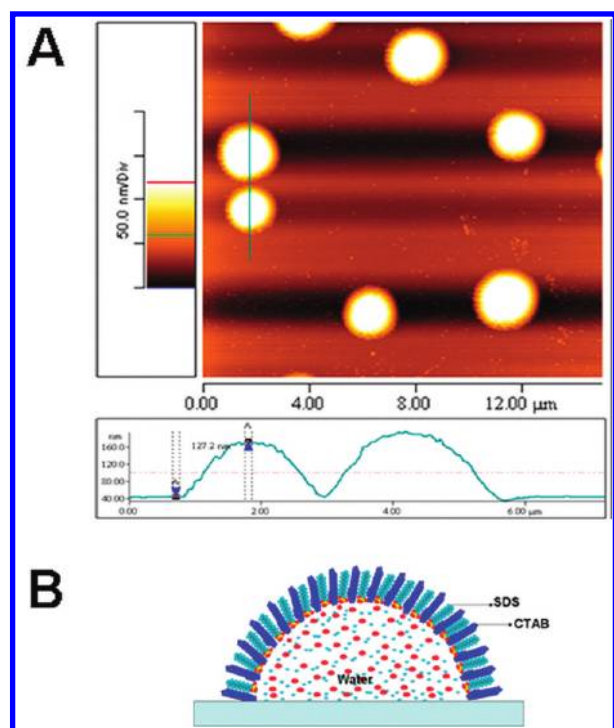
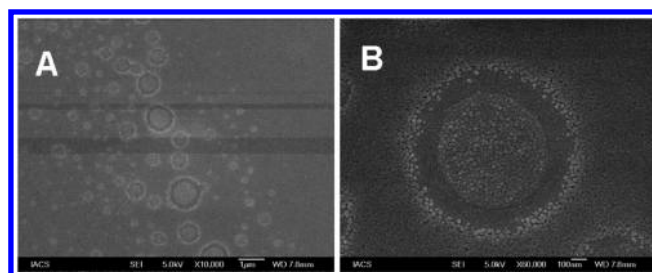


**Figure 5.** (A) AFM image of the LB film of SDS/CTAB (35/65) deposited on a glass substrate at a pressure of 20 mN/m. The graph at the bottom shows the height profile of the indicated line. The side bar is a color representation of height. (B) Cartoon of the hill-like three-dimensional structure.

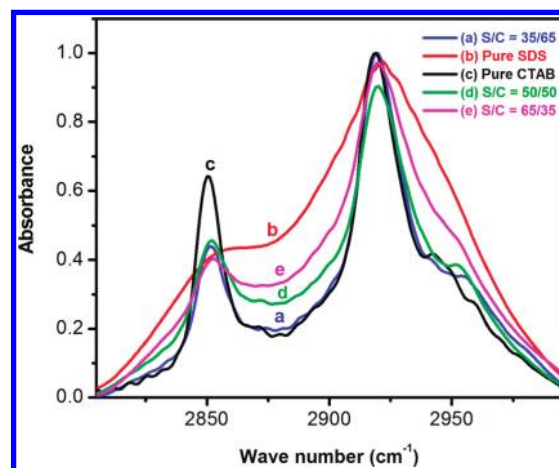
some three-dimensional assemblies that are stable at the air/water interface. For this reason, we chose this particular composition for detailed studies.

Figure 4A displays the change in  $\pi$ - $A$  isotherms of the SDS/CTAB = 35/65 catanionic mixture with waiting time. The growth of surface pressure with increasing waiting time shows that the electrostatic interaction between the oppositely charged head groups dominates over the area and tries to increase the pressure by organizing the molecules in a particular fashion. This can be related to Figure 1, where the surface pressure increases with time. Figure 4B presents a stability graph of the SDS/CTAB = 35/65 mixture at different surface pressures. In this figure, the relative area is plotted against time. The monolayer is less stable at higher surface pressure. This phenomenon illustrates the fact that the self-assembly of the molecules occurs at high pressure. At high surface pressure, the monolayer is more compressed. This implies that the molecules are closer to each other, initiating different types of interactions to form organized assemblies and hence trying to reduce the surface pressure. As a result, the area per molecule decreases to maintain the surface pressure.

**3.2. AFM and FE-SEM Images of Langmuir Monolayer Film.** We transferred the monolayers onto a glass substrate. Some interesting surface morphology was observed by AFM and FE-SEM. An AFM image recorded for a monolayer LB film of SDS/CTAB = 35/65 on a hydrophilic glass substrate at pressure 20 mN/m revealed some hill-like formations at the air/water interface (Figure 5A). The diameters of the hills were in the range of 1–2  $\mu\text{m}$ , and heights of these aggregates were in the range of 120–150 nm. To the best of our knowledge, these types of aggregates have been reported very rarely. According to Ghosh et al.,<sup>40</sup> the aggregates are vesicles, which contradicts the basic



**Figure 6.** FE-SEM images of the LB film of SDS/CTAB = 35/65 lifted at 20 mN/m on a glass substrate at different magnifications.



**Figure 7.** FTIR spectra in the C–H stretching region of pure SDS, pure CTAB, and catanionic mixtures.

structural property of vesicles. The outer layer of the vesicles is made of hydrophilic head groups; thus, the water medium is necessary for the existence of a spherical vesicular structure. In contrast, in LB films, the water medium is absent, and the film cannot contain spherical vesicles. According to our observations, the hill-like nature might arise from the dragging of water by hydrophilic head groups. In Figure 5B, a schematic cartoon of this hill type of three-dimensional structure is presented.

For the FE-SEM images, the LB monolayer film of SDS/CTAB = 35/65 was lifted at  $\pi$  = 20 mN/m onto a hydrophilic glass substrate. In the FE-SEM images, ring-type formations were observed (Figure 6). The origin of this type of morphology is not clear. However, it might be that, because of a vacuum, the water present inside the structure might evaporate, thus leaving the impressions of those hills. The dimensions of the structures observed by AFM were quite similar to those visualized by FE-SEM, which further supports the conclusion that this type of surface micelle morphology forms in LB films (SDS/CTAB = 35/65).

**3.3. FTIR Study of Pure and Catanionic Mixtures.** It is generally known that the frequencies of  $\text{CH}_2$  stretching modes are conformation-sensitive and can be empirically correlated with the conformational order (trans/gauche ratio) of alkyl chains.<sup>41,42</sup> To examine the conformational order of the interaction between SDS and CTAB, we recorded FTIR spectra of pure and mixed-surfactant systems, as displayed in Figure 7. From this figure, two peaks at 2850 and 2918  $\text{cm}^{-1}$  are observed. These two stronger bands are for symmetric [ $\nu_s(\text{CH}_2)$ ] and antisymmetric [ $\nu_a(\text{CH}_2)$ ]  $\text{CH}_2$  stretching modes of the alkyl chains of CTAB.<sup>43</sup> For SDS, the corresponding bands were observed at 2851 and 2922  $\text{cm}^{-1}$ ,



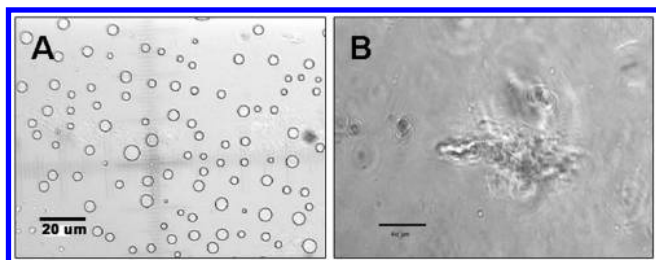


**Figure 8.** PCIM images of SDS/CTAB in water films with compositions of (A) 35/65 and (B) 90/10.

respectively, as reported by Kawai et al.<sup>19</sup> Figure 7 shows the antisymmetric  $\text{CH}_2$  stretching band,  $\nu_a(\text{CH}_2)$ , shifted for the SDS + CTAB catanionic mixed system. The frequencies of  $\nu_a(\text{CH}_2)$  for mixed-surfactant systems were in the range of  $2919\text{--}2920\text{ cm}^{-1}$ , between those for the pure-surfactant systems at  $2922$  and  $2918\text{ cm}^{-1}$ . This range is characteristic of highly ordered conformations with preferential all-trans characteristics, whereas a frequency of  $2922\text{ cm}^{-1}$  is characteristic of the melting of methylene chains, in which a number of gauche conformers exist.<sup>19,41,42</sup> Thus, these results indicate that the alkyl chains of the mixed-surfactant systems of SDS + CTAB are in the all-trans conformation (i.e., the solid state), whereas those in pure SDS or CTAB are in a fused state.

**3.4. PCIM Images of Aggregates in Water Film and at the Air/Water Interface.** Drops of catanionic aqueous solutions of different compositions were placed on hydrophilic glass slides and covered with fine glass coverslips, to form thin water films. Figure 8 shows PCIM images of some structures of spherical vesicles along with some unorganized aggregates. The SDS/CTAB composition of 35/65 exhibits a vesicular morphology (Figure 8A), whereas for other mixtures, some unorganized aggregates were observed. Figure 8B shows such unorganized aggregates for the composition of SDS/CTAB = 90/10. In general, lipids form vesicles because they have two hydrocarbon chains and, therefore, the packing parameters favor the formation of vesicles.<sup>43</sup> In contrast, pure surfactants (CTAB, SDS) have single hydrocarbon chains and have a tendency to form micelles.<sup>44</sup> However, in this case, two surfactants having oppositely charged head groups were mixed to form a catanionic mixture. In the mixture, the cationic and anionic groups neutralize each other to decrease their free energy and behave like bitail lipid molecules, as shown in Figure 2, and can form catanionic vesicles.<sup>44</sup>

In Figure 8A, each vesicle appears as dark circular rings, which originate from the variation of the opacity of the optical beam.<sup>45</sup> The opacity is greater where the vesicle bilayer is parallel to the optical beam and lower where the bilayer is perpendicular to the optical beam.<sup>40</sup> These are unilamellar vesicles, but the width of the dark rim is greater than the actual bilayer thickness. This mismatch arises because of the curvature of the vesicles.<sup>45</sup> O'Connor et al. also found vesicular solutions in this region.<sup>46</sup>

To pursue our interest in the aggregation phenomena of different catanionic compositions, we performed *in situ* imaging of the self-assemblies of different catanionic mixtures at the air/water interface. The solutions of binary systems of SDS and CTAB in organic solvent were spread at the air/water interface, and *in situ* images were recorded by PCIM at the micrometer scale after 10 min. Figure 9 shows the results for different compositions of SDS/CTAB. For SDS/CTAB ratios from 35/65 to 65/35, the figure shows circular types of organized aggregates

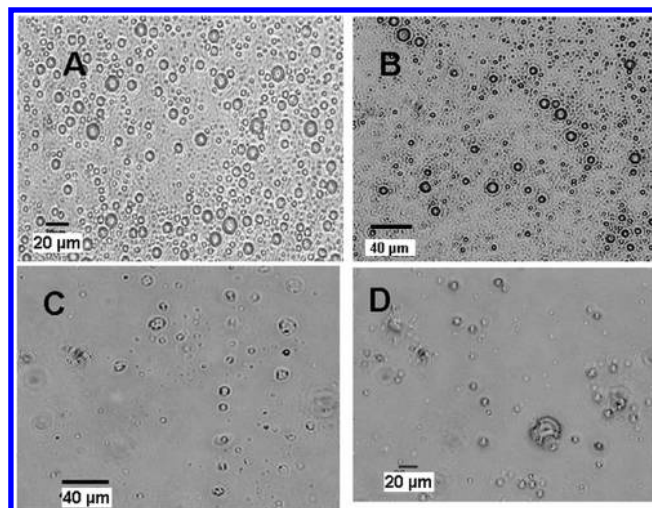


**Figure 9.** PCIM images of catanionic surfactants with various compositions of SDS/CTAB at the air/water interface: SDS/CTAB = (A) 35/65, (B) 65/35, (C) 90/10, and (D) 10/90.

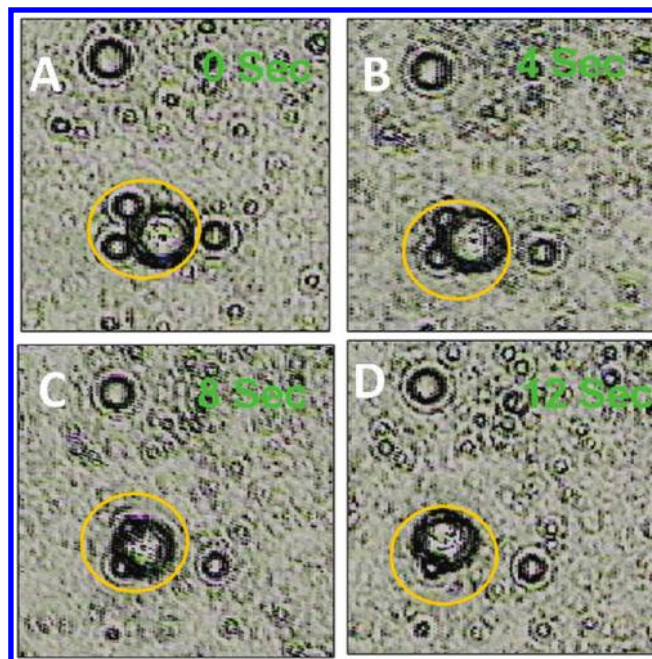


**Figure 10.** Time-dependent PCIM images showing the fusion of circular structures at the air/water interface. The yellow ring indicates the region of interest.

(Figure 9A,9B), whereas in 90/10 or 10/90 compositions, we found aggregates of irregular shapes (Figure 9C,9D). The organized structures might be catanionic surface micelles, having hydrophobic tails in the air and hydrophilic heads in water. They might form hemispherical structures at the air/water interface because of the pulling of water by the hydrophilic head groups. The AFM images (Figure 5A,5B) also illustrate this phenomenon. As the dimensions of the surface micelles are different, the focusing of each structure is very difficult. Because of the variation in height, when the larger ones are in focus, the smaller ones become defocused. That is why some structures in Figure 9 are defocused.

Parts A–D of Figure 10 sequentially display the growth of a catanionic surface micelle by fusion with a smaller one. Figure 9C,9D also shows that extremely anionic- and cationic-rich binary mixtures cannot form organized structures. This phenomenon also suggests that vesicle formation occurred for SDS/CTAB ratios between 35/65 and 65/35.

#### 4. CONCLUSIONS

Our study on SDS/CTAB mixtures both at the air/water interface and in aqueous solution shows strong electrostatic interactions between the oppositely charged head groups of the cationic and anionic surfactants. The aggregation behavior varies with the composition (relative amounts) of the SDS/CTAB systems. We observed the formation of catanionic surface micelles at the air/water interface with SDS/CTAB ratios in the range from 35/65 to 65/35 (volume ratio). On the other hand, in aqueous solution, spherical vesicles formed at the same compositions. For the remaining compositions (90/10, 10/90), unorganized aggregated morphologies were observed. An in situ time-dependent study of surface micelle formation at the air/water interface showed micelle ripening through the fusion of smaller micelles. Still, more detailed studies of the dynamic process of the growth of aggregates and different types of interactions responsible for different morphologies are needed and are in progress in our laboratory.

#### ■ ASSOCIATED CONTENT

**S** Supporting Information. Pressure–area ( $\pi$ – $A$ ) isotherms of pure CTAB after different waiting times. This information is available free of charge via the Internet at <http://pubs.acs.org>.

#### ■ AUTHOR INFORMATION

##### Corresponding Author

\*Tel.: +91-33-24734971. Fax: +91-33-24732805. E-mail: [spgbt@iacs.res.in](mailto:spgbt@iacs.res.in)

#### ■ ACKNOWLEDGMENT

We thank DST, Government of India (Project SR/S2/CMP-0051/2006) for partial financial support. M.M. thanks CSIR, Government of India, for providing the CSIR-NET fellowship. We also thank the Apex Instruments Co., Kolkata, India, for providing access to their PCIM fitted with MINI-LB2006C.

#### ■ REFERENCES

- (1) Rosen, M. J. *Surfactants and Interfacial Phenomena*; 3rd ed.; Wiley Interscience: New York, 2004.
- (2) Hentze, H.-P.; Raghavan, S. R.; McKelvey, C. A.; Kaler, E. W. *Langmuir* **2003**, *19*, 1069.
- (3) Guo, X.; Szoka, F. C. *Acc. Chem. Res.* **2003**, *36*, 335.
- (4) Maiti, K.; Mitra, D.; Mitra, R. N.; Panda, A. K.; Das, P. K.; Rakshit, A. K.; Moulik, S. P. *J. Phys. Chem. B* **2010**, *114*, 7499.
- (5) Karaborni, S.; Esselink, K.; Hilbers, P. A. J.; Smit, B. *J. Phys.: Condens. Matter* **1994**, *6*, A351.
- (6) Chen, I. A.; Walde, P. *Cold Spring Harb. Perspect. Biol.* **2010**, *2*, a002170.
- (7) Xu, Y.-X.; Wang, G.-T.; Zhao, X.; Jiang, X.-K.; Li, Z.-T. *Soft Matter* **2010**, *6*, 1246.
- (8) Kume, G.; Gallotti, M.; Nunes, G. J. *Surfactants Deterg.* **2008**, *11*, 1.
- (9) Chakraborty, H.; Sarkar, M. *Langmuir* **2004**, *20*, 3551.
- (10) Panda, A. K.; Possmayer, F.; Petersen, N. O.; Nag, K.; Moulik, S. P. *Colloids Surf. A* **2005**, *264*, 106.
- (11) Herrington, K. L.; Kaler, E. W.; Miller, D. D.; Zasadzinski, J. A.; Chiruvolu, S. *J. Phys. Chem.* **1993**, *97*, 13792.
- (12) Sohrabi, B.; Gharibi, H.; Tajik, B.; Javadian, S.; Hashemianzadeh, M. *J. Phys. Chem. B* **2008**, *112*, 14869.
- (13) Tanford, C. *The Hydrophobic Effect Formation of Micelles and Biological Membranes*; Wiley-Interscience: New York, 1980.
- (14) Khan, A.; Marques, E. In *Specialist Surfactants*; Robb, I. D., Ed.; Blackie Academic and Professional: London, 1997; pp 37–80.
- (15) P. Jokela, B. J.; Khan, A. *J. Phys. Chem.* **1987**, *91*, 3291.
- (16) Kondo, Y. U.; H.; Yoshino, N.; Nishiyama, K.; Abe, M. *Langmuir* **1995**, *11*, 2380.
- (17) Rodriguez, J.; Clavero, E.; Laria, D. *J. Phys. Chem. B* **2005**, *109*, 24427.
- (18) Groot, R. D.; Rabone, K. L. *Biophys. J.* **2001**, *81*, 725.
- (19) Kawai, T.; Yamada, Y.; Kondo, T. *J. Phys. Chem. C* **2008**, *112*, 2040.
- (20) Joy, S.; Pal, P.; Mahato, M.; Talapatra, G. B.; Goswami, S. *Dalton Trans.* **2010**, *39*, 2775.
- (21) Katsuhiko, A.; Hill, J. P.; Lee, M. V.; Vinu, A.; Charvet, R.; Acharya, S. *Sci. Technol. Adv. Mater.* **2008**, *9*, 014109.
- (22) Roefzaad, M.; Kluner, T.; Brand, I. *Phys. Chem. Chem. Phys.* **2009**, *11*, 10140.
- (23) Coppock, J. D.; Krishan, K.; Dennin, M.; Moore, B. G. *Langmuir* **2009**, *25*, 5006.
- (24) Mahato, M.; Pal, P.; Kamilya, T.; Sarkar, R.; Talapatra, G. B. *J. Phys. Chem. B* **2010**, *114*, 495.
- (25) Mahato, M.; Pal, P.; Kamilya, T.; Sarkar, R.; Chaudhuri, A.; Talapatra, G. B. *Phys. Chem. Chem. Phys.* **2010**, *12*, 12997.
- (26) Kamilya, T.; Pal, P.; Mahato, M.; Talapatra, G. B. *Mater. Sci. Eng. C* **2009**, *29*, 1480.
- (27) Kamilya, T.; Pal, P.; Talapatra, G. B. *Biophys. Chem.* **2010**, *146*, 85.
- (28) Kamilya, T.; Pal, P.; Mahato, M.; Talapatra, G. B. *J. Phys. Chem. B* **2009**, *113*, 5128.
- (29) Wang, Y.; Pereira, C. M.; Marques, E. F.; Brito, R. O.; Ferreira, E. S.; Silva, F. *Thin Solid Films* **2006**, *515*, 2031.
- (30) Lee, Y.-L.; Yang, Y.-C.; Shen, Y.-J. *J. Phys. Chem. B* **2005**, *109*, 4662.
- (31) Lin, J.; Nakagawa, M.; Uchiyama, K.; Hobo, T. *Chromatographia* **1999**, *50*, 739.
- (32) Cifuentes, A.; Bernal, J. L.; Diez-Masa, J. C. *Anal. Chem.* **1997**, *69*, 4271.
- (33) Dey, S.; Mandal, U.; Sen Mojumdar, S.; Mandal, A. K.; Bhattacharyya, K. *J. Phys. Chem. B* **2010**, *114*, 15506.
- (34) Vautier-Giongo, C.; Bales, B. L. *J. Phys. Chem. B* **2003**, *107*, 5398.
- (35) Zhao, F.; Xu, J. *Colloid Polymer Science* **2006**, *285*, 113.
- (36) Kaler, E. W.; Herrington, K. L.; Murthy, K. A.; Zasadzinski, J. A. *N. J. Phys. Chem.* **1992**, *96*, 6698.
- (37) Viseu, M. I.; Gonçalves da Silva, A. I. M.; Costa, S. M. B. *Langmuir* **2001**, *17*, 1529.
- (38) Pal, P.; Dutta, A. K.; Pal, A. J.; Misra, T. N. *Langmuir* **1994**, *10*, 2339.
- (39) Vaknin, D.; Bu, W. *J. Phys. Chem. Lett.* **2010**, *1*, 1936.
- (40) Ghosh, A.; Choudhury, S.; Das, A. *Chem.—Asian J.* **2010**, *5*, 352.
- (41) Umehura, J. M.; H. H.; Cameron, D. G. *J. Colloid Interface Sci.* **1981**, *83*, 558.
- (42) Kawai, T. U.; J.; Takenaka, T. *Colloid Polym. Sci.* **1984**, *262*, 61.
- (43) Kung, K. H. S.; Hayes, K. F. *Langmuir* **1993**, *9*, 263.
- (44) Salkar, R. A.; Mukesh, D.; Samant, S. D.; Manohar, C. *Langmuir* **1998**, *14*, 3778.
- (45) Jung, H. T.; Coldren, B.; Zasadzinski, J. A.; Iampietro, D. J.; Kaler, E. W. *Proc. Natl. Acad. Sci. U.S.A.* **2001**, *98*, 1353.
- (46) O'Connor, A. J.; Hatton, T. A.; Bose, A. *Langmuir* **1997**, *13*, 6931.